Available online at www.sciencedirect.com

ScienceDirect

Cite this article as: Rare Metal Materials and Engineering, 2018, 47(8): 2365-2370.

ARTICLE

Crack Growth Driving Force at Tip of Stress Corrosion Cracking in Nuclear Structural Materials at Initial Stage

Xue He,   Cui Yinghao,   Li Gangbo,   Wang Shuai

Xi'an University of Science and Technology, Xi'an 710054, China

Abstract: The mechanical state at the crack tip is one of the major factors affecting the stress corrosion cracking (SCC) growth rate in structural materials of the nuclear power plant. To understand the crack growth driving force and its effect on SCC growth rate in the whole process of SCC, a finite element model of the SCC growth process was built using a commercial software ABAQUS. Sequentially the working load, residual stress, and the film induced stress (FIS) produced by the oxide film formation in front of the crack tip during SCC initial stage were discussed in this paper. The results indicate that the FIS produced by the formation of oxide film is the main crack growth driving force during the initial stage of SCC. While the working load and residual stress gradually become the main crack growth driving force as SCC crack advances.

Key words: SCC; initial stage of crack; film induced stress; elastic-plastic finite element method

---

Stress corrosion cracking (SCC) is one of the important life degradation modes of nuclear power structural materials under high temperature and high pressure aqueous environments[1,2]. It is a type of slow crack growth process in materials that occurs under the combination of local mechanics, corrosion environment and material at the crack tip[3]. Considering the selection of nuclear power structural material, safe operation and life prediction etc, SCC growth rate is the most important factor of SCC research. To simplify the mechanical state at the crack tip and accelerate the experiment process, most of the SCC experiments are carried out using standard fracture mechanics specimen in an autoclave that simulates working environment in nuclear power plant[4].

Owing to the dense oxide film formed on its surface, nuclear structural material, such as stainless steel and nickel base alloy, is a strong anti-corrosion materials. And the defect area will quickly produce oxide film when surface "scratches" are induced by some disturbances in the surface structures material[5], whose main component is Cr_2O_3[6]. Film rupture model is one of the most main SCC propagation rate prediction models in nuclear structural materials, which

is proposed by Ford and Andresen and is known as the F-A model[7,8]. SCC propagation process is a film rupture, electrochemical reaction and repetitive process at the tip of SCC. This can be used to describe the crack initiation-small crack propagation and the crack accelerated extended life cycle[9]. As a matter of fact, a crack initial stage and short crack stage occupies most of SCC crack propagation time[10,11]. For the surface scratch and micro crack stage, external load including working load and residual stress has little mechanical effect on the SCC growth rate, but experiments showed that SCC growth rate is still growing slowly. Without external load, the formation of chromium-rich material and oxide film at the crack tip will induce wedge effect on the crack tip, resulting in the rupture of oxide film and the crack further extending into the base metal. This free-stress corrosion cracking can also be called film induced stress cracking[12]. The relevant experiment results showed that the surface stress of 304 stainless steel smooth specimen is about 30 MPa[13,14]. Li and Qian[15,16] found that the FIS and thermal stress are due to oxide film growth and temperature variation in the high temperature water environment, which is sufficient to cause the rupture

---

of oxide film and extend to the base metal. Nelson et al.[12] and Lu et al.[17] measured the variation of film induced stress with time and the stress in the interface of the oxide and base metal. Guo[18] et al. used the flow stress difference method to measure film induced stress at the crack tip caused by the formation of the oxide film.

Since the initial stage of SCC has great influence on the life cycle of the key structural materials in nuclear power plants, it is necessary to study the crack driving force in SCC life cycle. The finite element model of SCC crack initiation stage was established in this paper, and the change of crack driving force and crack propagation rate in SCC initial stage was studied.

1　Theoretical Basis

Ford and Andresen proposed a predicted model of SCC growth rate according to slip-dissolution/oxidation model, in which the SCC growth rate is expressed as follows[6-9]:

$$\frac{da}{dt} = \frac{M}{z\rho F} \cdot \frac{i_0}{1-m} \cdot \left(t_0\right)^m \cdot \left(\frac{\dot{\varepsilon}_{ct}}{\varepsilon_f}\right)^m \tag{1}$$

where, M and ρ are atomic mass and density of the metal, respectively. z is the charge due to the oxidation process, F is Faraday's constant, i_0 is the oxide current density in bare metal surface, m is the current decay index, t_0 is the initial time of current decay, ε_f is the oxide film rupture strain at crack tip and ε_{ct} is the crack tip strain rate.

The rupture of film at the crack tip is characterized by the plastic strain reaching the rupture strain of the oxide film at the crack tip. The crack tip strain ε_p is usually substituted by tensile strain at a characteristic distance r_0 from the crack tip, which is written as follows[19]:

$$\varepsilon_p = \varepsilon_{ct}\big|_{r=r_0} \tag{2}$$

where ε_p is the plastic strain at a characteristic distance r_0 from the crack front, and substituting Eq. (2) into Eq. (1), the SCC propagation rate can be written as Eq. (3):

$$\frac{da}{dt} = \frac{M}{z\rho F} \cdot \frac{i_0}{1-m} \cdot \left(t_0\right)^m \cdot \left(\frac{\dot{\varepsilon}_p}{\varepsilon_f}\right)^m \tag{3}$$

2　FEM Model

2.1　Geometric and mesh model

A finite wide plate, tensile specimen with a single edge crack is selected to simulate this process. The plate width is 80 mm and length is 160 mm, as shown in Fig.1a. The SCC initial growth process can be expressed as three stages, which are surface scratch, micro crack and small crack. To characterize different crack growth stages and study the change of the crack driving force and its effect on the crack growth rate, the crack length a is assumed as surface scratch, 5, 50, 200 and 2000 μm, respectively. To improve the analytical precision at the crack tip, the submodel technique is employed to calculate distribution of the stress-strain field at the crack tip. The 8-node
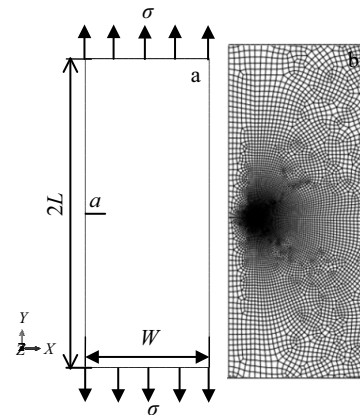

Fig.1　Finite element mesh and geometric model: (a) geometric model and (b) global mesh model

biquadratic plane strain element is adopted in ABAQUS, with total number of the global model mesh 18 424, as shown in Fig.1b. The element type of the submodel consistent with the whole model, and the minimum size of the element is about 0.05 μm in the submodel. To analyze the stress and strain field at the crack tip in SCC initial stage, two observation paths are defined nearby the crack tip region, one is the horizontal direction along crack tip and the other is a ring path with a distance from the crack tip, as shown in Fig.2.

2.2　Material mechanics model

The SCC crack tip morphology of austenitic stainless steel in high temperature and high pressure aqueous environments is shown in Fig.3, which is observed using ATEM[6]. In Fig.3, the white region is the oxide film. The base metal in this study is nickel-based alloy 600, which is classified as the power hardening material. The relationship between the stress and strain of the power hardening material can be described by Ramberg-Osgood equation[20].

$$\frac{\varepsilon}{\varepsilon_0} = \frac{\sigma}{\sigma_0} + \alpha\left(\frac{\sigma}{\sigma_0}\right)^n \tag{4}$$
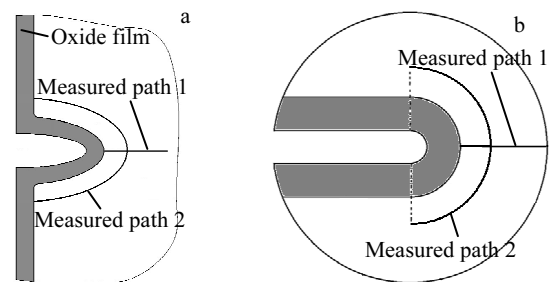

Fig.2　Measured path at crack tip region: (a) surface scratch and (b) other crack lengths
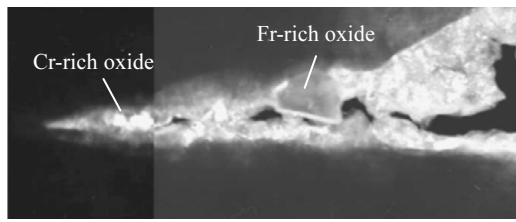
Fig.3   Microscopic morphology of SCC crack tip

Material mechanical parameters of nickel-based alloy 600 are: Young's modulus E 190 GPa, Poisson's ratio ν 0.3, yield stress $\sigma_{0.2}$ 436 MPa, strain hardening exponent n 5.29 and the offset coefficient α 1[21].

The main component of oxide film is Cr_2O_3, which is generally simplified as a linear elastic material, and its Young's modulus E is 19 GPa, Poisson's ratio ν is 0.3[22].

3   Results and Discussion

3.1   Tensile stress of crack tip at SCC initial stage

To understand the effect of the FIS on the stress field of the crack tip at SCC initial growth stage, the SCC crack lengths are assumed as surface scratch, 5, 50, 200 and 2000 μm in this study. To evaluate the effect of oxide film thickness on the FIS, the film thickness d was chosen as 1 μm[22].

The variation of tensile stress at different SCC stages is illustrated in Fig.4, which shows that the tensile stress decreases as the distance increases from the crack tip. The tensile stress is the largest during surface scratch period, which indicates tensile stress close to the crack tip is the main driving force of the film rupture. At the distance of 0.8 μm from crack tip, where tensile stress is lower than that of 2000 μm crack, it shows that crack tip stress is greater at surface scratch stage and its effect range of the crack tip is smaller than that of the long crack. From the surface scratch to the crack length of a=2000 μm, the calculation of the tensile stress along path 1 shows that it causes the tensile stress of the crack tip to decrease by 53%.
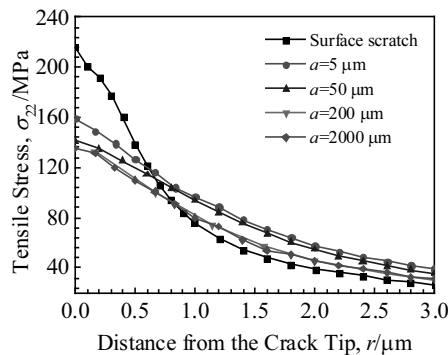
3.2   Contribution of FIS to crack tip tensile stress during initial stage

To understand the tensile stress at the crack tip under a combined effect of external load and FIS, an external load is applied by a specified external tensile stress σ in specimen, shown in Fig.1. The external loads include residual stresses and working loads, and the value of σ is 53 MPa, which is calculated by the stress intensity factor equal to 5 MPa·m$^{0.5}$ when the crack length is 2000 μm.

At the surface scratch stage, the tensile stress along path 2 under external load and combined effect of FIS and external load is shown in Fig.5, which also shows the ratio of FIS. Fig.5 shows that the biggest tensile stress appears in the 0° position. The tensile stress is 40 MPa only under external load, and its value rises to 110 MPa when FIS is also considered. Here the growth rate is 63%, which indicates that FIS accounts for a considerable proportion of the overall stress value at the surface scratch stage. Therefore, the contribution of FIS to the tensile stress is important and can not be ignored at the surface scratch stage

The tensile stress along path 2 under external load and combined effect of FIS and external load when crack length a=5 μm is shown in Fig.6, which also shows the ratio of FIS. The tensile stress is 72 MPa only under external load in the 0° position, and its value rises to 120 MPa when FIS is considered. The growth rate is 42%, which accounts for almost half of the overall stress. Therefore, the contribution of FIS to the tensile stress is also very large, and can not be ignored in the micro crack stage

The distribution of tensile stress along path 2 when crack length a=50 μm is shown in Fig.7, which is similar to the crack size of 5 μm. The stress growth rate at crack tip is 17% when compared with that of only simple external load, which shows that the tensile stress produced by FIS is less than the tensile stress produced by external load. The stress in the crack initiation stage has a certain influence on the stress at the crack tip.

The tensile stress distribution along path 2 when the crack length a=200 μm is shown in Fig.8. Maximum tensile stress at

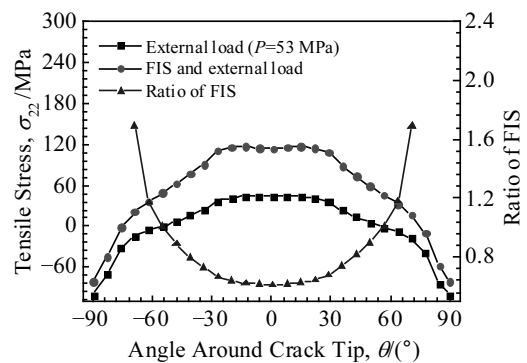Fig.4   Tensile stress produced by FIC along path 1

Fig.5   Tensile stress under FIS, external load and combined effect (surface scratch)
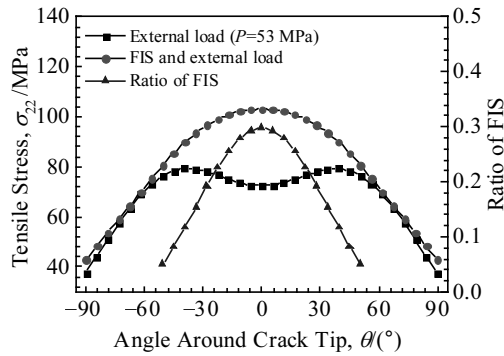
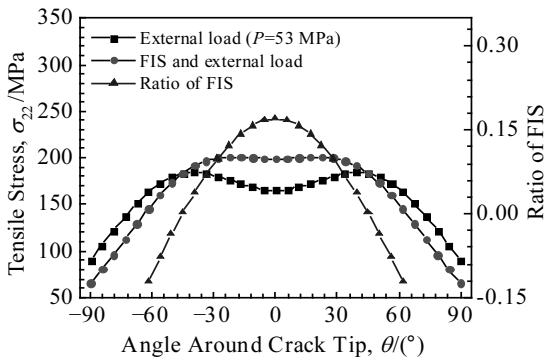Fig.6   Tensile stress under FIS, external load and combined effect (*a*=5 μm)

Fig.7   Tensile stress under FIS, external load and combined effect (*a*=50 μm)

crack tip also appears in the 0° position, and becomes steep in the vicinity of the stress range. This shows that, the effect of film induced stress on crack tip region of 0° is more obvious at the micro crack stage. The stress growth rate increases by about 11% after the addition of film induced stress, which shows that the effect of FIS on the tensile stress is small, and can be ignored at the crack tip.
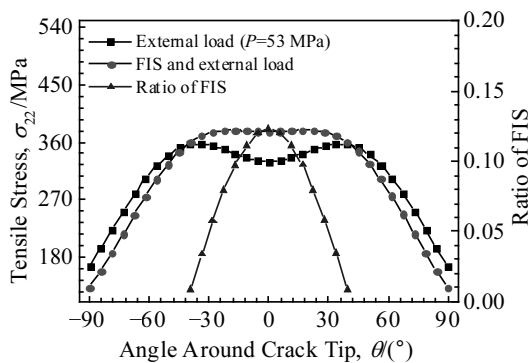

Fig.8   Tensile stress under FIS, external load and combined effect (*a*=200 μm)

The tensile stress distribution along path 2 when crack length *a*=2000 μm is shown in Fig.9. The value of maximum tensile stress at crack tip is 920 MPa in the 0° direction only under constant external loading. Moreover its value rises to 960 MPa when film induced stress is also considered. Here the growth rate in stress is 4%. Therefore, the contribution of FIS to the tensile stress is small, and isn't significantly detectable on the stress at the crack tip.

3.3   Tensile stress produced by FIS at crack tip under combined effect of load

The proportion of the tensile stress at crack tip produced by FIS among the whole crack propagation driving force is shown in Fig.10. It can be seen intuitively that the contribution of the FIS decreases gradually with the increasing crack propagation length. At the surface scratch stage, the contribution ratio is 63% when crack is surface scratch, and the ratio is 42% when the crack size is 5 μm. Compared with 4% at *a*=2000 μm, the gap between them is very large. Compared with crack lengths *a*=50 μm, *a*=200 μm and *a*=2000 μm, the proportion of the tensile stress accounts for 50% of the total stress at crack tip when the crack size *a*=5 μm.

3.4   Influence of various loads on crack growth rate

The effect of stress at the SCC initial stage is very large. During the crack initiation stage, the driving force of SCC
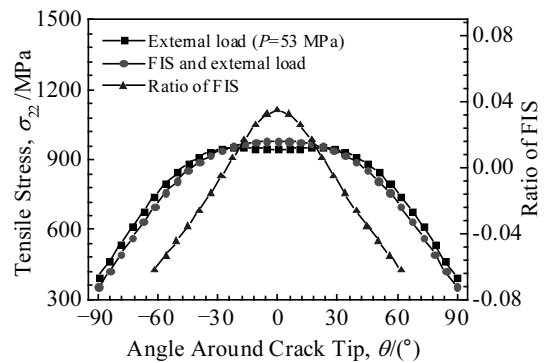

Fig.9   Tensile stress under FIS, external load and combined effect (*a*=2000 μm)
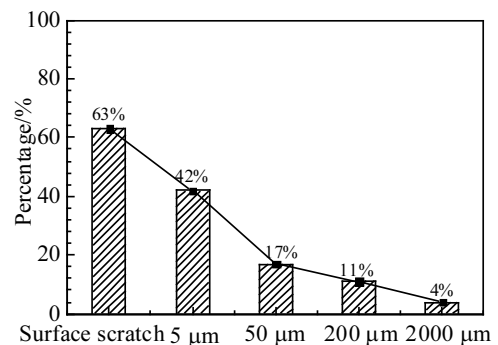

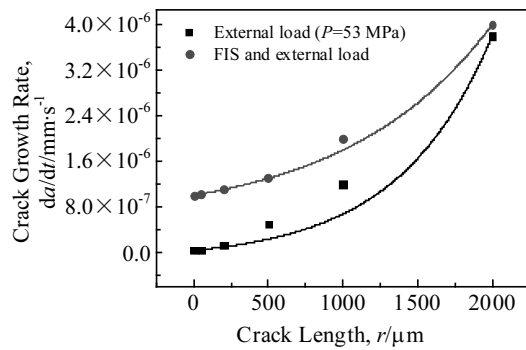Fig.10   Percentage of tensile stress produced by FIS at crack tip

Fig.11 Combined effect of FIS and constant load on crack growth law in different crack lengths

Table 1 Water chemistry material parameters of Alloy 600[19,23]

Parameter	Value
Atomic mass, M/g·mol^{-1}	55
Number of equivalents exchanged, z	2.67
Oxidization current density, i_0/A·mm^{-2}	0.00015
Fracture strain of oxide film, ε_f	0.0025
Exponent of current decay curve, m	0.4
Faraday's constant, F/C·mol^{-1}	96500
Duration of constant i_0, t_0/s	0.4
Density, ρ/g·mm^{-3}	0.00786

crack propagation is mainly FIS.

When the material of base metal is constant, tensile stress at crack tip determines the plastic strain rate and the driving force of SCC crack propagation. Fig.11 shows the plastic strain rate ε_p at a crack tip with the characteristic distance of r_0=4 μm. The crack growth rate was observed under both cases: i.e. external load and combined effect of FIS and external load. This was calculated using Eq. (3). The water chemistry parameter of alloy 600 in high temperature water environment is shown in Table 1.

It can be seen from Fig.11 that the crack propagation rate under the combined effect of load and FIS is much larger than that of under only external load at the crack initiation stage. It shows that the FIS plays an important role in crack growth rate at this stage and it is also the main driving force of crack propagation. The crack growth rate tends to be similar under the two kinds of loads, and eventually becomes the same with the growth of cracks. It can be concluded that the contribution of the external load to the crack growth rate constantly increases at the long cracking stage, and becomes the main driving force of crack propagation at this stage. From the whole SCC and crack growth diagram, the crack growth rate increases slowly at the crack initiation stage. With the increasing of crack length, the crack growth rate increases exponentially until the oxide ruptures.

4 Conclusions

1) At the surface scratch stage, tensile stress is lower than

that of 2000 μm crack, which shows that crack tip tensile stress is greater in surface scratch and its effect range of the crack tip is smaller than that of the long crack. The shorter the crack is, the greater the effect on the FIS on the oxide film rupture is.

2) Film induced stress produced by the formation of oxide film is the main crack growth driving force at the initial stage of SCC, and its impact on the crack growth rate can not be ignored.

3) The contribution of the tensile stress to crack growth rate decreases gradually as SCC crack advances, while the contribution of the load to the SCC crack propagation rate gradually increases and becomes the main SCC driving force. Therefore, at the long crack stage, the film induced stress can be neglected in the SCC test using the standard fracture mechanics specimen.

References

1 Zinkle S J, Was G S. *Acta Materialia*[J], 2013, 61(3): 735
2 Peng Q J, Xue H, Hou J *et al. Corrosion Science*[J], 2011, 53(12): 4309
3 Xue H, Shoji T. *Journal of Pressure Vessel Technology*[J], 2007, 129(3): 460
4 Dong L J, Han E H, Peng Q J *et al. Corrosion Science*[J], 2017, 117: 1
5 Meng Fanjiang, Wang Jianqiu, Han Enhou *et al. Acta Metallurgica Sinica*[J], 2011, 47(7): 839 (in Chinese)
6 Lu Y H, Peng Q J, Sato T *et al. Journal of Nuclear Materials*[J], 2005, 347(1-2): 52
7 Ford F P. *International Journal of Pressure Vessels and Piping*[J], 1989, 40(5): 343
8 Andresen P L, Ford F P. *Materials Science and Engineering A*[J], 1988, 103(1): 167
9 Ford F P. *Corrosion Science*[J], 1996, 52(5): 375
10 Fang X R, Xue H, Yang F Q. *Rare Metal Materials and Engineering*[J], 2016, 45(2): 321
11 Qin Chenghua, Ye Shen, Zhang Xiancheng *et al. Materials for Mechanical Engineering*[J], 2016, 40(2): 11 (in Chinese)
12 Nelson J C, Oriani R A. *Corrosion Science*[J], 1993, 34(2): 307
13 Li Jinxu, Gao Kewei, Su Yanjing *et al. Science Sinica Technologica, Series E*[J], 2003, 33(9): 796 (in Chinese)
14 Li J X, Chu W Y, Wang Y B *et al. Corrosion Science*[J], 2003, 45(7): 1355
15 Li Meishuan, Xin Li, Qian Yuhai *et al. Corrosion Science and Protection Technology*[J], 1999, 11(5): 300 (in Chinese)
16 Qian Yuhai, Li Meishuan. *Corrosion Science and Protection Technology*[J], 2003, 15(2): 90 (in Chinese)
17 Lu H, Gao K W, Chu W Y. *Corrosion Science*[J], 1998, 40(10): 1663
18 Guo Xianzhong, Gao Kewei, Qiao Lijie *et al. Progress in Natural Science*[J], 2002, 12(4): 438 (in Chinese)
19 Xue H, Sato Y, Shoji T. *Journal of Pressure Vessel Technology*[J], 2009, 131(1): 61

20　Ramberg W, Osgood W R. *Description of Stress-Strain Curves by Three Parameters, NACA-TN-902*[R]. Washington, DC: NACA, 1943

21　Xue H, Li Y Q. *Rare Metal Materials and Engineering*[J], 2016, 45(3): 537

22　Xue He, Xue Xiaofeng, Tang Wei *et al. Rare Metal Materials and Engineering*[J], 2010, 40(7): 1188 (in Chinese)

23　Bruemmer S, Ford P, Was G. *Ninth International Symposium on Environmental Degradation of Materials in Nuclear Power Systems-Water Reactors*[C]. Indianapolis: John Wiley & Sons, 2013: 49

核电结构材料应力腐蚀开裂初始阶段裂尖驱动力的研究

薛　河，崔英浩，李岗博，王　帅

(西安科技大学，陕西 西安 710054)

摘　要：裂尖力学状态是影响核电结构材料应力腐蚀开裂(SCC)扩展速率的主要因素之一。为了研究 SCC 不同扩展阶段裂尖驱动力的变化及其对 SCC 扩展速率的影响，建立了 SCC 扩展不同阶段的有限元模型，详细分析了裂纹初始阶段影响裂尖应力状态的工作载荷、残余应力，以及氧化膜形成过程中产生的膜致应力。结果表明，在 SCC 裂纹初始阶段，裂尖氧化膜形成所产生的"镶入张力"是 SCC 的主要驱动力；随着裂纹的扩展，工作载荷和残余应力逐渐成为 SCC 裂纹扩展的主要驱动力。

关键词：SCC；初始裂纹；膜致应力；弹塑性有限元

作者简介：薛　河，男，1961 年生，博士，教授，西安科技大学机械工程学院，陕西 西安 710054，电话：029-85583159，E-mail: xuehe1961@163.com